# Universal Scaling Law for the Largest Lyapunov Exponent in Coupled Map Lattices

Weiming Yang
*Center for Complex Systems and Department of Mathematics, Florida Atlantic University, Boca Raton, Florida 33431*

E-Jiang Ding
*Chinese Center of Advanced Science and Technology (World Laboratory), P.O. Box 8730, Beijing 100080, People's Republic of China*
*and Institute of Low Energy Nuclear Physics, Beijing Normal University, Beijing 100875, People's Republic of China*

Mingzhou Ding*
*Center for Complex Systems and Department of Mathematics, Florida Atlantic University, Boca Raton, Florida 33431*
(Received 25 August 1995)

We consider coupled map lattices of the type $x_i(n+1) = (1-\epsilon)f(x_i(n)) + (\epsilon/2)[f(x_{i-1}(n)) + f(x_{i+1}(n))]$, where for concreteness we take $f(x) = 1 - (\mu/4)|1-2x|^p$, with $p > 1$. We show that near $\epsilon = 0$ (no coupling) and $\mu = 4$ the envelope of the largest Lyapunov exponent of the full system obeys the scaling law $\overline{\Lambda} = \Lambda_0 - [a\epsilon + b(4-\mu)]^{1/p}$. We further argue that this law is universal in that it is independent of the details of $f(x)$ insofar as $f(x)$ has a single critical point $x_c$ in the interval $[0,1]$ and its lowest order power expansion about $x_c$ has the form $|x - x_c|^p$. The dependence of $\overline{\Lambda}$ on the size of the lattice as well as on the range of the coupling is also discussed.

PACS numbers: 05.45.+b, 05.50.+q

Coupled map lattices (CMLs) [1], as discrete analogs to coupled oscillators and partial differential equations, have in recent years become the model of choice for developing intuitions and concepts in the study of spatiotemporal chaotic systems. Among the variety of quantities applied to characterize the dynamics of a CML, the spectrum of Lyapunov exponents stands out for its ease of numerical evaluation, and for the wealth of information that derives from it. For example, from Pesin's formula [2], the sum of all positive Lyapunov exponents provides an estimate of the Kolmogorov-Sinai entropy. Meanwhile, one obtains the information dimension of the chaotic attractor by employing the Kaplan-Yorke conjecture [3]. Moreover, the largest Lyapunov exponent (LLE), denoted henceforth by $\Lambda$, quantifies the sensitive dependence on initial conditions, a hallmark of chaos [4], by yielding the rate of exponential divergence of two typical nearby trajectories.

In this Letter we focus on the scaling behavior of $\Lambda$ near certain limiting situations. Consider a diffusively coupled map lattice of the form

$$x_i(n+1) = (1-\epsilon)f(x_i(n)) + (\epsilon/2) \times [f(x_{i-1}(n)) + f(x_{i+1}(n))], \quad (1)$$

where $n$ denotes the discrete time, $i$ labels the lattice site, $f(x)$ prescribes the local dynamics, and $\epsilon$ gives the coupling strength. For ease of presentation we assume $f(x) = 1 - (\mu/4)|1-2x|^p$ with $p > 1$. That is, the local map has one critical point ($x_c = 1/2$) in [0,1] and the maximum at $x_c$ is of the $p$th order. For $p = 2$ we get the logistic map. When $\mu = 4$ the function $f(x)$ is surjective, mapping the interval [0,1] onto itself. Our main result in this Letter is that, for Eq. (1), near $\epsilon = 0$ and $\mu = 4$, the envelope [5] of $\Lambda$, denoted $\overline{\Lambda}$, scales with $\epsilon$ and $4 - \mu$ as

$$\overline{\Lambda} = \Lambda_0 - [a\epsilon + b(4-\mu)]^{1/p}, \quad (2)$$

where $\Lambda_0$ is the Lyapunov exponent of $f(x)$ at $\mu = 4$. We emphasize that, although Eq. (2) is formulated in terms of a specific class of $f(x)$, the scaling law appears to be universal in the sense that its form is independent of the details of $f(x)$ provided that $f(x)$ is unimodal with one critical point $x_c$ in [0,1] and the maximum at $x_c$ is of the $p$th order. It is interesting to note that both in the present problem and in the problem of period doubling cascade studied by Feigenbaum [6], the universality classes are delineated by the same exponent $p$. In what follows we establish Eq. (2) by combining numerical and analytical techniques. Other related works are listed in [7–11].

*Numerical results.*—First, consider the case of $\epsilon = 0$. In the absence of coupling all the Lyapunov exponents have the same value $\Lambda = \lim_{N\to\infty}(1/N)\sum_{n=1}^{N} \ln|f'(x_n)|$ where $x_{n+1} = f(x_n)$. Near $\mu = 4$ and for $p = 2$, it is found in [7] that $\overline{\Lambda}$ scales with $4 - \mu$ as $\overline{\Lambda} = \Lambda_0 - \alpha(4-\mu)^{1/2}$. Based on numerical evidence we now extend this result to general $p$ values, namely,

$$\overline{\Lambda} = \Lambda_0 - \alpha(4-\mu)^{1/p}. \quad (3)$$

In Figs. 1(a) and 1(b) we verify this relation by plotting $\Lambda$ as a function of $(4-\mu)^{1/p}$ for $p = 2$ and $p = 1.5$. It can be seen that both data sets show linear trends conforming with Eq. (3). The slopes of the straight line fits give $\alpha_1 = 0.50$ in Fig. 1(a) and $\alpha_2 = 0.41$ in Fig 1(b). Similar calculations for other values of $p$ and for different maps within the same $p$ class are carried out and they all show excellent agreement with Eq. (3).

 0031-9007/96/76(11)/1808(4)$10.00 

Next, we examine the case of $\mu = 4$. Let $L$ be the lattice size and take the boundary condition to be periodic. Unless specified otherwise we use $L = 100$ throughout for computation. Numerical simulations in [9] suggest that for $\epsilon$ small,

$$\overline{\Lambda} = \Lambda_0 - \beta \epsilon^{1/p}. \tag{4}$$

In Figs. 2(a) and 2(b) we present the plots of $\Lambda$ vs $\epsilon^{1/p}$ for $p = 2$ and $p = 1.5$. Excellent agreement between the data and Eq. (4) is evident. The slopes of the straight fits yield $\beta_1 = 0.65$ in Fig. 2(a) and $\beta_2 = 0.63$ in Fig. 2(b).

Rewrite Eqs. (3) and (4) as $(\Lambda_0 - \overline{\Lambda})^p = \alpha^p(4 - \mu)$ and $(\Lambda_0 - \overline{\Lambda})^p = \beta^p \epsilon$, respectively. These two equations hint at the supposition that $(\Lambda_0 - \overline{\Lambda})^p$ is an analytic function in both variables $\epsilon$ and $4 - \mu$. Assuming this is so and expanding the function to the lowest order in $\epsilon$ and $4 - \mu$, we have $(\Lambda_0 - \overline{\Lambda})^p = a\epsilon + b(4 - \mu)$, or, equivalently, $\overline{\Lambda} = \Lambda_0 - [a\epsilon + b(4 - \mu)]^{1/p}$, which is Eq. (2). Clearly, $a$ and $b$ relate to $\alpha$ and $\beta$ as $a = \alpha^p$ and $b = \beta^p$. We perform numerical experiments to test Eq. (2) for the case of both $\epsilon \neq 0$ and $4 - \mu \neq 0$. Specifically, let us take a straight line in the plane spanned by $\epsilon$ and $4 - \mu$, say, for simplicity, $\epsilon = 4 - \mu$. Then we calculate $\Lambda$ along this line. Equation (2) predicts that the plot of $\Lambda$ vs $\epsilon^{1/p}$ is a straight line with the slope of $-(a + b)^{1/p} = -(\alpha^p + \beta^p)^{1/p}$ where $\alpha$ and $\beta$ are from the $\epsilon = 0$ case and the $4 - \mu = 0$ case, respectively. The result for $p = 2$ is presented in Fig. 3(a). The straight line fit has a slope of $-0.78$ which agrees reasonably well with the predicted slope of $-(\alpha_1^p + \beta_1^p)^{1/p} = -0.82$. In Fig. 3(b) we show the result for $p = 1.5$. The value of the slope of the linear tendency in the data points is $-0.83$ which is again close to the prediction $-(\alpha_2^p + \beta_2^p)^{1/p} = -0.81$. These two examples, together with numerous other numerical experiments not included here, establish the validity of the scaling law in Eq. (2).

From the foregoing discussion we see that Eqs. (3) and (4) are the foundation for the conjecture in Eq. (2). While the inspiration for Eq. (3) comes from [7], we are able to obtain a heuristic derivation for Eq. (4), which we present below. Some basic steps of this derivation are outlined in [10]. See also [11] for a random matrix approach to a class of CMLs in which the local map has strictly positive derivatives.

*Theoretical results.*—To evaluate $\Lambda$ we examine the variations along a typical given chaotic orbit [12], $\{\mathbf{x}(n)\}_{n=1}^{\infty}$, in the $L$-dimensional phase space. From Eq. (1) we have

$$\begin{aligned}\delta x_i(n+1) = (1-\epsilon) f'(x_i(n))\delta x_i(n) + (\epsilon/2) \\ \times [f'(x_{i-1}(n))\delta x_{i-1}(n) \\ + f'(x_{i+1}(n))\delta x_{i+1}(n)].\end{aligned} \tag{5}$$

Let $\mathbf{A}(n)$ denote the $L \times L$ Jacobian matrix at the orbit point $\mathbf{x}(n)$. From Eq. (5), its elements are $a_{i,i}(n) = (1-\epsilon)f'(x_i(n))$, $a_{i,i-1}(n) = (\epsilon/2)f'(x_{i-1}(n))$, and $a_{i,i+1}(n) = (\epsilon/2)f'(x_{i+1}(n))$ for $2 \le i \le L-1$. The elements $a_{1,1}(n)$, $a_{1,2}(n)$, $a_{L,L-1}(n)$, and $a_{L,L}(n)$ are formed in the same way, and the periodic boundary condition adds $a_{1,L}(n) = (\epsilon/2)f'(x_L(n))$ and

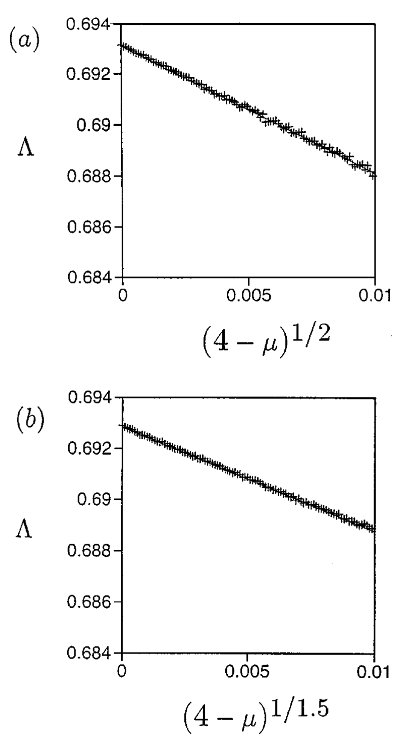


FIG. 1. Plots of (a) $\Lambda$ vs $(4 - \mu)^{1/2}$ for $p = 2$ and (b) $\Lambda$ vs $(4 - \mu)^{1/1.5}$ for $p = 1.5$. Here $\epsilon = 0$.

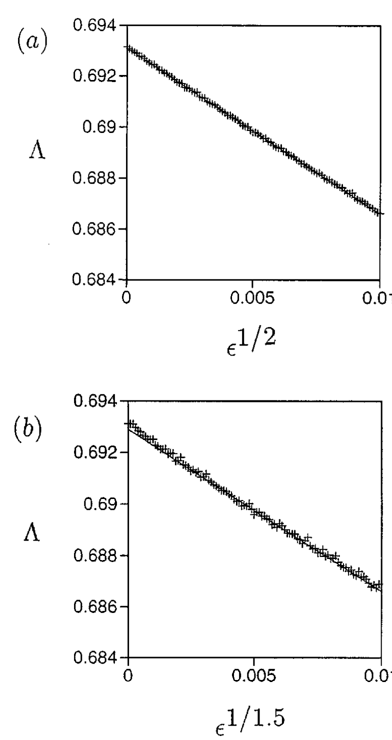


FIG. 2. Plots of (a) $\Lambda$ vs $\epsilon^{1/2}$ for $p = 2$ and (b) $\Lambda$ vs $\epsilon^{1/1.5}$ for $p = 1.5$. Here $\mu = 4$.

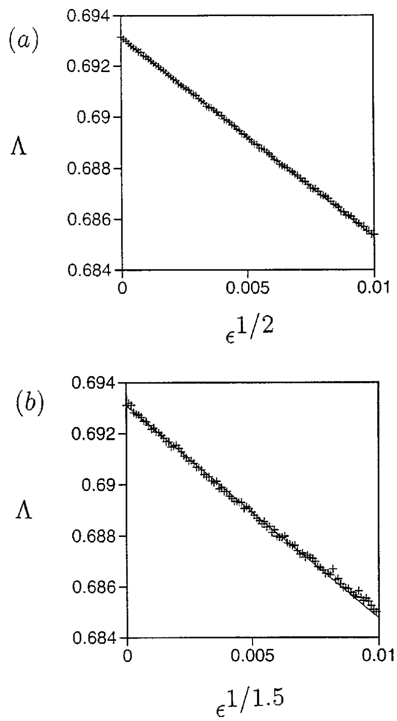


FIG. 3. Plots of (a) $\Lambda$ vs $\epsilon^{1/2}$ for $p = 2$ and (b) $\Lambda$ vs $\epsilon^{1/1.5}$ for $p = 1.5$. Here $\epsilon = 4 - \mu$.

$a_{L,1}(n) = (\epsilon/2)f'(x_1(n))$. In other words we treat $i = 0$ as equivalent to $i = L$. All the other matrix elements are zero.

Let $\mathbf{T}^{(N)} = \mathbf{A}(N)\mathbf{A}(N-1)\cdots\mathbf{A}(1)$. Then, the LLE of the CML can be expressed as

$$\Lambda = \lim_{N\to\infty}(1/N)\ln|\mathrm{tr}\mathbf{T}^{(N)}|, \tag{6}$$

where tr denotes trace. The $i$th diagonal element of $\mathbf{T}^{(N)}$ is

$$t_{i,i}^{(N)} = \sum_{j_N,\ldots,j_2} a_{i,j_N}(N)a_{j_N,j_{N-1}}(N-1)\cdots a_{j_2,i}(1). \tag{7}$$

For large $L$ most of $a_{k,l}(n)$ are zero except those with $|k-l| \le 1$. Keep in mind that if we say $k = 1$ then $l = 0$ is used in the place of $l = L$.

Now let us imagine a two-dimensional space-time lattice in which a point $(i,n)$, where $1 \le i \le L$ and $1 \le n < \infty$, is used to index the state of the $i$th space site at time $n$. Because of the periodic boundary condition this space-time lattice lies on the surface of a semi-infinite cylinder. Furthermore, every nonzero product in the sum Eq. (7) corresponds to a "path" from $(i,1)$ to $(i,N)$ in the lattice, denoted $r$, where the intermediate steps $(j_2,2)$, $(j_3,3),\ldots,$ and $(j_{N-1},N-1)$ satisfy $|j_2 - i| \le 1$, $|j_3 - j_2| \le 1,\ldots,$ and $|i - j_N| \le 1$. In this product, each term, besides the variable $f'(x)$, contributes a factor $\epsilon/2$ if $|j_k - j_{k-1}| = 1$, a factor $1-\epsilon$ otherwise. Thus, along a given path $r$, the total number of $\epsilon/2$ is $m(r) = |j_2 - i| + |j_3 - j_2| + \cdots + |i - j_N|$. Equation (7) becomes $t_{i,i}^{(N)} = \sum_r (1-\epsilon)^{N-m(r)}(\epsilon/2)^{m(r)}\prod_{n,j\in r} f'(x_j(n))$. To further facilitate the evaluation of $t_{i,i}^{(N)}$, the dynamics are assumed to be independent temporally at the same lattice site [13], and are also independent spatially at different lattice sites. This is a reasonable approximation given that the coupling is weak ($\epsilon \to 0$) and the parameter $\mu$ is near maximum chaos ($\mu \to 4$). For large $N$, based on the independence assumption, we replace $|\prod_{n,j\in r} f'(x_j(n))|$ computed along each possible path $r$ by the same $|\prod_n f'(x_i(n))|$ evluated at the $i$th lattice site. Since $f'(x)$ can be either positive or negative, by introducing a random variable $q_r = \pm 1$, we write approximately

$$t_{i,i}^{(N)} = \Big|\prod_n f'(x_i(n))\Big|\sum_r q_r(1-\epsilon)^{N-m(r)}(\epsilon/2)^{m(r)}. \tag{8}$$

Viewing the sum in the above equation as a random walk with nonuniform steps we argue that $\lim_{N\to\infty}(1/N)\ln[\sum_r q_r(1-\epsilon)^{N-m(r)}(\epsilon/2)^{m(r)}]$ is a quantity of $O(\epsilon)$ order. Thus, the task of estimating the LLE for the CML, Eq. (6), is reduced to that for a single map, i.e.,

$$\begin{aligned}\Lambda &= \lim_{N\to\infty}(1/N)\ln\Big|\prod_n f'(x(n))\Big| + O(\epsilon)\\ &= \int_0^1 \ln|f'(x)|\rho_\epsilon(x)\,dx + O(\epsilon),\end{aligned} \tag{9}$$

where we have dropped the reference to $i$ since all the lattice points are equivalent. To evaluate the integral in Eq. (9) we need the characteristic of the invariant density $\rho_\epsilon(x)$ which we discuss below.

It suffices to consider $L = 3$ since the invariant density at a given lattice site is determined mainly by its own dynamics and that of its two nearest neighbors. We begin with the case of $p = 2$. The local map is $x_{n+1} = 4x_n(1-x_n)$. When $\epsilon = 0$ the invariant density is known to be $\rho_0(x) = 1/\pi\sqrt{x(1-x)}$, which is singular at $x = 0$ and $x = 1$. We argue that these singularities are removed in the presence of coupling. In particular, $\rho_\epsilon(0) = \rho_\epsilon(1) = 0$ for $\epsilon \ne 0$. To see this, refer to Eq. (1). Consider the map at the first lattice site and the interval $1 - \eta < x_1 < 1$ where $\eta \ll \epsilon$. The invariant measure contained in the interval is $\int_{1-\eta}^1 \rho_\epsilon(x_1)\,dx_1$. To have $x_1(n+1) \in (1-\eta, 1)$, the values of $x_i(n)$, $i = 1,2,3$, need to lie roughly in intervals of width $\sim\sqrt{\eta}$ centered around $1/2$. The probability to achieve that is $\sim\eta^{3/2}$. Thus, $\int_{1-\eta}^1 \rho_\epsilon(x_1)\,dx_1 = \rho_\epsilon(\xi)\eta \sim \eta^{3/2}$, where $1-\eta < \xi < 1$. Letting $\eta \to 0$ yields $\rho_\epsilon(1) = 0$. Similar arguments lead to $\rho_\epsilon(0) = 0$. In a future longer paper a more complete picture of the qualitative behavior of $\rho_\epsilon(x)$ will be established. Its three major features can be summarized as follows (see Fig. 4). (1) When $\epsilon < x < 1 - \epsilon$, $\rho_\epsilon(x) = 1/C\sqrt{x(1-x)}$, where $C$ is determined by normalization. (2) At $x \sim \epsilon$ or $x \sim 1 - \epsilon$, $\rho_\epsilon$ reaches its local maximal values, $\rho_\epsilon \sim 1/\sqrt{\epsilon}$. (3) As $x$ increases from $1-\epsilon$ to 1 or decreases from $\epsilon$ to 0, $\rho_\epsilon \to 0$. Note that $\rho_\epsilon(x)$ is no longer symmetric with respect to $x_c = 1/2$ as is the case when $\epsilon = 0$.

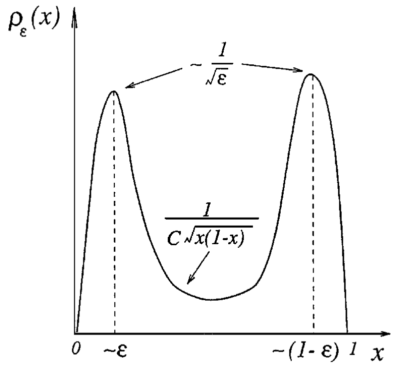


FIG. 4. Schematic of the qualitative behavior of the invariant density $\rho_\epsilon(x)$.

Equipped with this understanding of $\rho_\epsilon(x)$ we proceed with the calculation of $\Lambda$ in Eq. (9). Namely, $\Lambda = \int_0^1 \ln|4 - 8x|\rho_\epsilon(x)\,dx + O(\epsilon) = \int_0^1 \ln|4 - 8x|\{(\pi/C)\rho_0(x) - [(\pi/C)\rho_0(x) - \rho_\epsilon(x)]\}\,dx + O(\epsilon) \approx (\pi/C)\times \Lambda_0 - \ln 4 \int_0^1[(\pi/C)\rho_0(x) - \rho_\epsilon(x)]\,dx + O(\epsilon) = (\pi/C)\Lambda_0 - (\pi/C - 1)\ln 4 + O(\epsilon) = \Lambda_0 + (\pi/C - 1)\times(\Lambda_0 - \ln 4) + O(\epsilon)$, where we have utilized the facts that $(\pi/C)\rho_0(x)$ and $\rho_\epsilon(x)$ essentially coincide in the range $\epsilon < x < 1 - \epsilon$ and that $\rho_0(x)$ and $\rho_\epsilon(x)$ are both normalized. The order of magnitude of $\pi/C - 1$ is estimated to be $\pi/C - 1 = \int_0^1[(\pi/C)\rho_0(x) - \rho_\epsilon(x)]\,dx \sim \int_0^\epsilon dx/x^{1/2} \sim \epsilon^{1/2}$. Hence,

$$\Lambda - \Lambda_0 \sim \epsilon^{1/2}, \tag{10}$$

where quantities of $O(\epsilon)$ order or higher are neglected.

For general values of $p$ we use $f_p(x) = 1 - |1 - 2x|^p$ with $p > 1$ as the representative local map. When $\epsilon = 0$, the invariant density $\rho_0(x)$ again has singularities at $x = 0$ and $x = 1$. In particular, $\rho_0(x) \sim x^{(1/p-1)}$ for $x \to 0$ and $\rho_0(x) \sim (1 - x)^{(1/p-1)}$ for $x \to 1$. When $\epsilon \neq 0$ is small, the same schematic in Fig. 4 describes the behavior of $\rho_\epsilon(x)$, except that now at $x \sim \epsilon$ and $x \sim 1 - \epsilon$, $\rho_\epsilon \sim \epsilon^{(1/p-1)}$. Following similar steps as in the $p = 2$ case we get

$$\Lambda - \Lambda_0 \sim \int_0^\epsilon x^{(1/p-1)}\,dx + O(\epsilon) \sim \epsilon^{1/p}. \tag{11}$$

We make two remarks. First, the preceding heuristic arguments rely on the qualitative behavior of $\rho_\epsilon(x)$, some order-of-magnitude estimates associated with it, and rather drastic assumptions about the behavior of the Jacobian matrix. Such results are not affected by the detailed properties of $f(x)$ such as the location of the critical point. This leads us to conjecture that the scaling law Eq. (4) is universal for unimodal maps with a single $p$th order maximum. Numerical simulations provide further support for this claim and enable us to extend it to include Eq. (2).

Second, in Eq. (1), nearest-neighbor coupling is assumed for the CML. Our approach above, particularly the concept of the space-time lattice, still applies if the coupling extends beyond the nearest neighbors. In this case, although more paths need to be included in the sum in Eq. (7), we again end up calculating $\Lambda$ from Eq. (9). The character of $\rho_\epsilon(x)$ is now much more difficult to assess. But there is reason to believe that similar qualitative behavior in Fig. 4 is still applicable here. Numerical evidence indeed indicates that Eq. (2) holds for couplings of wider range. Another important parameter in a coupled system is its size. For the present work the question is how $\Lambda$ asymptotes its thermodynamic-limit value as $L \to \infty$. Our preliminary result shows that $\overline{\Lambda(L) - \Lambda(\infty)} \sim 1/L$ for large $L$. This result, together with Eq. (2), provides a complete scaling description of the behavior of the largest Lyapunov exponent $\Lambda$ in coupled map lattices near the point $(\epsilon, \mu, L) = (0, 4, \infty)$.

This work is supported by a grant from the Office of Naval Research. E. J. D.'s work is also supported by the National Natural Science Foundation of China.

*To whom correspondence should be addressed.

[1] See, for example, K. Kaneko, Chaos **2**, 279 (1992), and other articles in this special focus issue on coupled map lattices.
[2] Ya B. Pesin, Dokl. Akad. Nauk. **226**, 774 (1976).
[3] J. L. Kaplan and J. A. Yorke, in *Functional Differential Equations and Approximations of Fixed Points*, edited by H.-O. Peitgen and H.-O. Walter, Lecture Notes in Mathematics Vol. 730 (Springer, Berlin, 1979), p. 204.
[4] E. Ott, *Chaos in Dynamical Systems* (Cambridge University Press, Cambridge, 1993).
[5] Mathematically, we can speak only about the scaling behavior of the envelope of $\Lambda$ as there are possibly infinitely many parameter combinations near $\epsilon = 0$ and $\mu = 4$ for which the system exhibits periodic attractors.
[6] M. J. Feigenbaum, J. Stat. Phys. **19**, 160 (1978).
[7] P. Collet and J.-P. Eckmann, *Iterated Maps on the Interval as Dynamical Systems* (Birkhauser, Boston, 1980), p. 33.
[8] H. Daido, Prog. Theor. Phys. **72**, 853 (1984); F. Kaspar and H. G. Schuster, Phys. Lett. **113A**, 451 (1986); S. P. Kuznetsov and A. S. Pikovsky, Physica (Amsterdam) **19D**, 384 (1986); T. Bohr, G. Grinstein, Y. He, and C. Jayaprakash, Phys. Rev. Lett. **58**, 2155 (1987); T. Bohr and O. B. Christensen, Phys. Rev. Lett. **63**, 2161 (1989); S. Isola, A. Politi, S. Ruffo, and A. Torcini, Phys. Lett. A **143**, 365 (1990); E. J. Ding and Y. N. Lu, J. Phys. A **25**, 2897 (1992); H. Chaté, Europhys. Lett. **21**, 419 (1993); Z. Qu and G. Hu, Phys. Rev. E **49**, 1099 (1994).
[9] E. J. Ding and Y. N. Lu, Phys. Lett. A **161**, 357 (1992).
[10] W. M. Yang, Chaos, Solitons Fractals **1**, 389 (1991).
[11] R. Livi, A. Politi, and S. Ruffo, J. Phys. A **25**, 4813 (1992).
[12] This assumption means that the following derivation for $\Lambda$ is oblivious to the possible presence of periodic windows. Thus the $\Lambda$ scaling so obtained can be viewed as representing the behavior of $\overline{\Lambda}$ defined earlier.
[13] Further justification for this assumption can be found in C. Beck, Nonlinearity **4**, 1131 (1991).